热力工程

文章编号: 1001 - 2060(2016) 07 - 0062 - 06

利用抽汽蓄能提高机组调频能力的定量分析

张锐锋[1], 练海晴[2], 田　亮[3]
(1. 贵州电力试验研究院, 贵州 贵阳 550002; 2. 国网新疆电力公司昌吉供电公司, 新疆 昌吉 831100;
3. 华北电力大学 控制与计算机工程学院, 河北 保定 071003)

摘　要: 合理利用凝结水系统蓄能能够提高机组发电负荷响应速率, 定量分析其蓄能容量对优化控制系统设计及保证机组安全运行意义重大。依据质量、能量守恒定律, 结合等效焓降法计算凝结水流量变化与各加热器抽汽流量、比焓以及汽轮机功率变化之间的对应关系, 再依据除氧器容积计算得到蓄能总量。600 MW、1 000 MW 典型机组的计算结果表明: 该方法具有较高的准确度; 同一机组凝结水系统蓄能容量随负荷增加而增加; 运行参数越高的机组凝结水系统的蓄能容量越大。

关　键　词: 火电机组; 凝结水系统; 蓄能容量; 负荷调节; 焓降

中图分类号: TP273　　**文献标识码:** A

DOI: 10.16146/j.cnki.rndlgc.2016.07.010

引　言

电网期望火电机组 AGC(发电负荷指令) 响应速率能够达到机组额定负荷的 2%/min 以上, 实际大部分机组与这一目标存在差距[1~2]。火电机组的协调控制对象具有大惯性、大迟延特性, 单纯依靠改变燃料量响应机组负荷指令速度非常缓慢, 需合理利用机组蓄能来提高负荷响应速度[3~4]。现有的机跟炉的协调控制系统, 则采用锅炉蓄热来提高机组负荷响应速率, 但会造成汽轮机前蒸汽压力波动。

凝结水系统蓄能利用的基本原理是: 利用低压加热器抽汽流量与凝结水流量之间的自平衡关系, 通过瞬时改变凝结水流量, 改变进入低压加热器的汽轮机抽汽流量, 进而改变机组发电功率。其本质上是利用了凝结水系统的蓄能。文献[5]在 900 MW 超临界机组上通过实验验证了凝结水系统蓄能调整发电负荷的可行性; 文献[1]分析了凝结水流量变化量与机组发电负荷变化量之间静态、动态对应关系; 文献[6]通过实验获得了凝结水流量与发电负荷之间的传递函数, 研究凝结水流量模糊自适应控制算法并应用于控制系统设计。

合理利用凝结水系统蓄能需要对凝结水系统蓄能容量进行定量分析。文献[1]为了简化计算, 只给出凝结水完全节流工况下发电负荷的变化量。现场中凝结水节流会导致除氧器水箱和凝汽器水箱水位大幅波动, 威胁机组运行安全。实际机组运行过程中不允许出现这种极端的情况, 需要分析凝结水流量在合理工况范围内变化时与机组发电负荷的对应关系。同时其计算方法也存在一定误差。

1　机理分析

典型的火电机组回热加热系统一般采用 4 低压加热器、1 除氧器、3 高压加热器的结构, 如图 1 所示。

根据图 1 建立各个加热器及除氧器的质量平衡和能量平衡方程:

对于 1、5 号加热器($i=1,5$), 有:

$$\frac{\mathrm{d}M_i}{\mathrm{d}t} = Q_{\mathrm{es},i} - Q_{\mathrm{sw},i} \tag{1}$$

$$\frac{\mathrm{d}E_i}{\mathrm{d}t} = Q_{\mathrm{es},i}(h_{\mathrm{es},i} - h_{\mathrm{sw},i}) - Q_{\mathrm{cw}}(h_{\mathrm{cw},i} - h_{\mathrm{cw},i+1}) \tag{2}$$

对于 2,3,6,7,8 号加热器($i=2,3,6,7,8$), 有:

$$\frac{\mathrm{d}M_i}{\mathrm{d}t} = Q_{\mathrm{es},i} + Q_{\mathrm{sw},i-1} - Q_{\mathrm{sw},i} \tag{3}$$

收稿日期: 2015 - 06 - 09;　修订日期: 2015 - 11 - 03
基金项目: 国家重点基础研究发展计划(973 计划) 资助项目(2012CB215203); 中央高校基本科研业务费专项资金资助(2014MS145)
作者简介: 张锐锋(1968 -), 男, 四川雅安人, 贵州电力试验研究院高级工程师.
通讯作者: 练海晴(1990 -), 女, 新疆奎屯人, 华北电力大学硕士研究生.

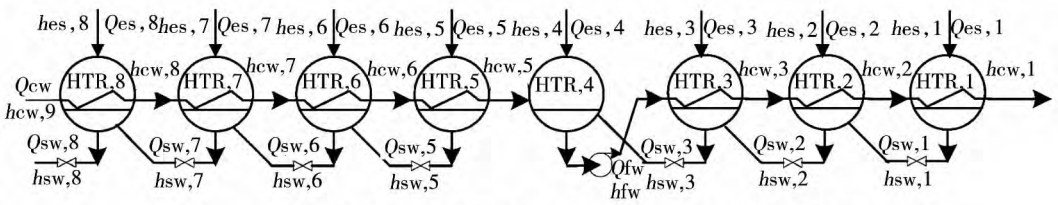

i–各个加热器编号（*i*=1、2、3...8）；HTR.*i*–各个加热器

图 1　典型回热加热系统流程图

Fig. 1 Flow chart of a typical recuperative heating system

$$\frac{\mathrm{d}E_i}{\mathrm{d}t} = Q_{\mathrm{es},i}(h_{\mathrm{es},i} - h_{\mathrm{sw},i}) + Q_{\mathrm{sw},i-1}(h_{\mathrm{sw},i-1} - h_{\mathrm{sw},i}) - Q_{\mathrm{cw}}(h_{\mathrm{cw},i} - h_{\mathrm{cw},i+1}) \tag{4}$$

对于 4 号加热器（$i=4$），有:

$$\frac{\mathrm{d}M_4}{\mathrm{d}t} = Q_{\mathrm{cw}} + Q_{\mathrm{es},4} + Q_{\mathrm{sw},3} - Q_{\mathrm{fw}} \tag{5}$$

$$\frac{\mathrm{d}E_4}{\mathrm{d}t} = Q_{\mathrm{cw}}h_{\mathrm{cw},5} + Q_{\mathrm{es},4}h_{\mathrm{es},4} + Q_{\mathrm{sw},3}h_{\mathrm{sw},3} - Q_{\mathrm{fw}}h_{\mathrm{fw}} \tag{6}$$

式中: M_i—各个加热器内壳侧汽水工质总质量，kg; E_i—各个加热器内壳侧汽水工质总能量，kJ; $Q_{\mathrm{es},i}$—各级抽汽流量，kg/s; $h_{\mathrm{es},i}$—各级抽汽比焓，kJ/kg; Q_{cw}—凝结水流量，kg/s; $h_{\mathrm{cw},i}$—流出各个加热器凝结水比焓，kJ/kg; $Q_{\mathrm{sw},i}$—各级疏水流量，kg/s; $h_{\mathrm{sw},i}$—各级疏水比焓，kJ/kg; Q_{fw}—给水流量，kg/s; h_{fw}—给水比焓，kJ/kg。

参考等效焓降法[7~8]，分析凝结水流量同各级抽汽流量之间的关系。

令:

$$\begin{cases} q_i = h_{\mathrm{es},i} - h_{\mathrm{sw},i}(i = 1,2,3,5,6,7,8) \\ \mathrm{q_i} = \mathrm{h_{es,i}} - \mathrm{h_{fw}}(\mathrm{i} = 4) \end{cases} \tag{7}$$

$$\tau_i = h_{\mathrm{cw},i} - h_{\mathrm{cw},i+1}(i = 1,2,\cdots 8) \tag{8}$$

$$\begin{cases} \gamma_i = h_{\mathrm{sw},i-1} - h_{\mathrm{sw},i}(i = 2,3,6,7,8) \\ \gamma_i = h_{\mathrm{sw},i-1} - h_{\mathrm{fw}}(i = 4) \end{cases} \tag{9}$$

式中: q_i—单位流量蒸汽放热量，kJ/kg; τ_i—单位流量给水焓升，kJ/kg; γ_i—单位流量疏水放热量，kJ/kg。

在静态工况下，式(1) ~(6)中左侧的微分项为零，将式(7) ~(9)代入质量平衡和能量平衡方程，令左侧等式为零。可得出各级抽汽流量同凝结水流量之间的对应关系:

$$Q_{\mathrm{es},1} = \alpha_1 Q_{\mathrm{fw}} = \frac{\tau_1}{q_1}Q_{\mathrm{cw}} \tag{10}$$

$$Q_{\mathrm{es},2} = \alpha_2 Q_{\mathrm{fw}} = \frac{\tau_2 - \alpha_1\gamma_2}{q_2}Q_{\mathrm{cw}} \tag{11}$$

$$Q_{\mathrm{es},3} = \alpha_3 Q_{\mathrm{fw}} = \frac{\tau_3 - (\alpha_1 + \alpha_2)\gamma_3}{q_3}Q_{\mathrm{cw}} \tag{12}$$

$$Q_{\mathrm{es},4} = \alpha_4 Q_{\mathrm{cw}} = \frac{\tau_4 - (\alpha_1 + \alpha_2 + \alpha_3)\gamma_4}{q_4}Q_{\mathrm{cw}} \tag{13}$$

$$Q_{\mathrm{es},5} = \alpha_5 Q_{\mathrm{cw}} = \frac{\tau_5}{q_5}Q_{\mathrm{cw}} \tag{14}$$

$$Q_{\mathrm{es},6} = \alpha_6 Q_{\mathrm{cw}} = \frac{\tau_6 - \alpha_5\gamma_6}{q_6}Q_{\mathrm{cw}} \tag{15}$$

$$Q_{\mathrm{es},7} = \alpha_7 Q_{\mathrm{cw}} = \frac{\tau_7 - (\alpha_5 + \alpha_6)\gamma_7}{q_7}Q_{\mathrm{cw}} \tag{16}$$

$$Q_{\mathrm{es},8} = \alpha_8 Q_{\mathrm{cw}} = \frac{\tau_8 - (\alpha_5 + \alpha_6 + \alpha_7)\gamma_8}{q_8}Q_{\mathrm{cw}} \tag{17}$$

式中: α_i—各级抽汽系数。

由上式中可以得出，在静态工况下，当抽汽、疏水、凝结水比焓保持不变时，4 ~ 8 号加热器的抽汽流量同凝结水流量成比例变化。在凝结水流量变化时，各级抽汽、凝结水、疏水温度压力变化很小[9~10]，因而其比焓变化也很小，为简便计算，认为抽汽系数不变，可得:

$$Q_{\mathrm{es},i} = \alpha_i Q_{\mathrm{cw}}(i = 4,5,6,7,8) \tag{18}$$

各个加热器对应的焓降分别为:

$$H_8 = h_{\mathrm{es},8} - h_{\mathrm{L}} \tag{19}$$

$$H_7 = h_{\mathrm{es},7} - h_{\mathrm{L}} - \frac{\gamma_8}{q_8}H_8 \tag{20}$$

$$H_6 = h_{\mathrm{es},6} - h_{\mathrm{L}} - \frac{\gamma_8}{q_8}H_8 - \frac{\gamma_7}{q_7}H_7 \tag{21}$$

$$H_5 = h_{\mathrm{es},5} - h_{\mathrm{L}} - \frac{\gamma_8}{q_8}H_8 - \frac{\gamma_7}{q_7}H_7 - \frac{\gamma_6}{q_6}H_6 \tag{22}$$

$$H_4 = h_{\mathrm{es},4} - h_{\mathrm{L}} - \frac{\tau_8}{q_8}H_8 - \frac{\tau_7}{q_7}H_7 - \frac{\tau_6}{q_6}H_6 - \frac{\tau_5}{q_5}H_5 \tag{23}$$

$$H_3 = h_{\mathrm{es},3} - h_{\mathrm{L}} - \frac{\tau_8}{q_8}H_8 - \frac{\tau_7}{q_7}H_7 - \frac{\tau_6}{q_6}H_6 - \frac{\tau_5}{q_5}H_5 - \frac{\gamma_4}{q_4}H_4 \tag{24}$$

$$H_2 = h_{es,2} - h_L - \frac{\tau_8}{q_8}H_8 - \frac{\tau_7}{q_7}H_7 - \frac{\tau_6}{q_6}H_6 - \frac{\tau_5}{q_5}H_5 - \frac{\gamma_4}{q_4}H_4 - \frac{\gamma_3}{q_3}H_3 \quad (25)$$

$$H_1 = h_{es,1} - h_L - \frac{\tau_8}{q_8}H_8 - \frac{\tau_7}{q_7}H_7 - \frac{\tau_6}{q_6}H_6 - \frac{\tau_5}{q_5}H_5 - \frac{\gamma_4}{q_4}H_4 - \frac{\gamma_3}{q_3}H_3 - \frac{\gamma_2}{q_2}H_2 \quad (26)$$

式中: H_i—焓降, kJ/kg; h_L—低压缸排汽比焓, kJ/kg。

当凝结水系统流量减少时,除氧器和 4 个低压加热器抽汽流量减少的部分将在汽轮机内做功,使机组发电功率增加[11]。

根据式(18)得出凝结水流量变化量与各级抽汽流量变化量成比例关系,为:

$$\Delta Q_{es,i} = \alpha_i \Delta Q_{cw} \quad (i = 4,5,6,7,8) \quad (27)$$

式中: $\Delta Q_{es,i}$—各级抽汽流量变化量, kg/s; ΔQ_{cw}—凝结水流量变化量, kg/s。

则机组发电功率增加:

$$\Delta N_E = \sum_{i=4}^{8} 0.001 \Delta Q_{es,i} H_i \quad (28)$$

将式(27)代入式(28)整理可得为:

$$\Delta N_E = \sum_{i=4}^{8} 0.001 \alpha_i H_i \Delta Q_{cw} \quad (29)$$

式中: ΔN_E—机组功率变化量, MW。

式(29)即为凝结水流量变化与机组功率变化之间的静态对应关系。

2 计算实例

2.1 600 MW 亚临界机组

以 PS 电厂 600 MW 亚临界机组为例进行定量分析,汽轮机型号为 N600 - 16.7/537/537。表 1 列出机组 100%、75% 和 50% THA(热耗考核)工况下回热系统热力性质参数。

根据表 1 中的数据可以得出 600 MW 机组在各工况下焓降的计算结果如表 2 所示。

表 1 600 MW 机组回热系统 THA 工况设计参数

Tab. 1 Design parameters of the recuperative system for a 600 MW unit under the THA operating condition

工况		1 号	2 号	3 号	4 号	5 号	6 号	7 号	8 号	低压缸
100% THA	h_{cw}/kJ·kg^{-1}	1 201.1	1 052.6	863.5	—	569.3	435.8	351.3	255.9	—
	h_{sw}/kJ·kg^{-1}	1 077.3	880.8	764.4	—	458.1	373.4	277.7	168.9	—
	h_{es}/kJ·kg^{-1}	3 126.6	3 013.9	3 325.5	3 147.0	2 948.2	2 761.9	2 640.8	2 510.0	—
	h_{fw}/kJ·kg^{-1}	—	—	—	725.9	—	—	—	—	—
	$h_{cw,9}$/kJ·kg^{-1}	—	—	—	—	—	—	—	142.4	—
	h_L/kJ·kg^{-1}	—	—	—	—	—	—	—	—	2 340.4
75% THA	h_{cw}/kJ·kg^{-1}	1 115.1	977.9	803.7	—	530	403.3	323.2	232.7	—
	h_{sw}/kJ·kg^{-1}	1 000.4	821	712.8	—	425.5	345.2	254.5	169.8	—
	h_{es}/kJ·kg^{-1}	3 140.7	3 025.6	3 291.7	3 119.2	2 926	2 744	2 626.4	2 499.1	—
	h_{fw}/kJ·kg^{-1}	—	—	—	676.7	—	—	—	—	—
	$h_{cw,9}$/kJ·kg^{-1}	—	—	—	—	—	—	—	142.4	—
	h_L/kJ·kg^{-1}	—	—	—	—	—	—	—	—	2 351.4
50% THA	h_{cw}/kJ·kg^{-1}	1 009.4	886.7	730.1	—	482.1	362.1	286.9	202.4	—
	h_{sw}/kJ·kg^{-1}	908.6	749	650	—	384.2	308.8	224.2	171.4	—
	h_{es}/kJ·kg^{-1}	3 165.1	3 048.1	3 296.4	3 127.3	2 934.9	2 750.2	2 631.5	2 506.8	—
	h_{fw}/kJ·kg^{-1}	—	—	—	617.5	—	—	—	—	—
	$h_{cw,9}$/kJ·kg^{-1}	—	—	—	—	—	—	—	142.4	—
	h_L/kJ·kg^{-1}	—	—	—	—	—	—	—	—	2 402.2

将表 2 中的数据代入式(29),可以得到 100%、75%、50% THA 工况凝结水流量变化对应机组功率变化的增益(以下简称增益)分别为 0.110 MJ/kg, 0.095 MJ/kg, 0.080 MJ/kg,随发电功率降低呈减小的趋势。

2.2　1 000 MW 超超临界机组

以 ZX 电厂 1 000 MW 超超临界机组为例进行分析,汽轮机型号为 N1000 – 25/600/600。表 3 中列出机组在 100%、70% 和 50% THA 工况下回热系统热力性质参数。

根据表 3 中的数据可以得出 1 000 MW 机组在 THA 工况下焓降的计算结果如表 4 所示。

表 2　600 MW 机组 THA 工况下焓降计算结果

Tab. 2 Calculation results of the enthalpy drop of a 600 MW unit under the THA operating condition

工况		1 号	2 号	3 号	4 号	5 号	6 号	7 号	8 号
100% THA	α	0.072 37	0.081 98	0.036 84	0.061 64	0.053 61	0.033 48	0.036 84	0.042 72
	H/kJ·kg^{-1}	623.2	557.6	908.4	769.1	574.0	401.8	292.5	169.6
75% THA	α	0.064 10	0.073 79	0.035 21	0.057 50	0.050 67	0.031 70	0.035 01	0.034 50
	H/kJ·kg^{-1}	644.4	572.6	873.7	711.8	546.5	377.0	269.7	147.7
50% THA	α	0.054 38	0.064 34	0.032 55	0.051 99	0.047 05	0.029 35	0.032 42	0.025 64
	H/kJ·kg^{-1}	642.2	561.8	840.2	679.9	514.3	340.0	229.3	104.6

表 3　1 000 MW 机组回热系统 THA 工况设计参数

Tab. 3 Design parameters of the recuperative system of a 1 000 MW unit under the THA operating condition

工况		1 号	2 号	3 号	4 号	5 号	6 号	7 号	8 号	低压缸
100% THA	h_{cw}/kJ·kg^{-1}	1 302.8	1 127.8	936.5	—	653.1	557.7	454.1	356.3	—
	h_{sw}/kJ·kg^{-1}	1 155.1	953.5	822.3	—	581.3	477.2	379.0	174.4	—
	h_{es}/kJ·kg^{-1}	3 198.8	3 064.9	3 463.7	3 245.8	3 095.2	2 953.0	2 798.9	2 656.4	—
	h_{fw}/kJ·kg^{-1}	—	—	—	810.7	—	—	—	—	—
	$h_{cw,9}$/kJ·kg^{-1}	—	—	—	—	—	—	—	151.9	—
	h_L/kJ·kg^{-1}	—	—	—	—	—	—	—	—	2 326.4
70% THA	h_{cw}/kJ·kg^{-1}	1 178.9	1 026.9	854.4	—	596.7	508.5	411.9	321.5	—
	h_{sw}/kJ·kg^{-1}	1 050.1	871.1	751.7	—	532.1	435.1	344.5	176.7	—
	h_{es}/kJ·kg^{-1}	3 240.5	3 105.1	3 467.8	3 249.7	3 093.6	2 949.4	2 793.6	2 652.6	—
	h_{fw}/kJ·kg^{-1}	—	—	—	738.6	—	—	—	—	—
	$h_{cw,9}$/kJ·kg^{-1}	—	—	—	—	—	—	—	154.0	—
	h_L/kJ·kg^{-1}	—	—	—	—	—	—	—	—	2 342.1
50% THA	h_{cw}/kJ·kg^{-1}	1 080.4	943.8	786.0	—	548.6	466.3	375.6	291.4	—
	h_{sw}/kJ·kg^{-1}	965.5	803.4	692.3	—	489.9	398.8	314.4	179.7	—
	h_{es}/kJ·kg^{-1}	3 277.7	3 139.9	3 471.1	3 253.9	3 093.7	2 948.5	2 791.9	2 652.7	—
	h_{fw}/kJ·kg^{-1}	—	—	—	677.3	—	—	—	—	—
	$h_{cw,9}$/kJ·kg^{-1}	—	—	—	—	—	—	—	156.7	—
	h_L/kJ·kg^{-1}	—	—	—	—	—	—	—	—	2 378.9

表 4　1 000 MW 机组 THA 工况下焓降计算结果

Tab. 4 Calculation results of the enthalpy drop of a 1 000 MW unit under the THA operating condition

工况		1 号	2 号	3 号	4 号	5 号	6 号	7 号	8 号
100% THA	α	0.085 63	0.082 43	0.039 28	0.063 73	0.037 95	0.040 25	0.037 24	0.072 84
	H/kJ·kg^{-1}	672.4	590.1	1038.0	823.9	699.3	581.0	445.3	330.0
70% THA	α	0.069 39	0.071 66	0.036 43	0.055 58	0.034 43	0.037 09	0.034 27	0.060 48
	H/kJ·kg^{-1}	720.8	632.6	1 039.0	825.3	692.5	570.2	430.2	310.5
50% THA	α	0.059 08	0.063 44	0.034 22	0.049 04	0.031 61	0.034 44	0.031 74	0.049 14
	H/kJ·kg^{-1}	744.0	648.5	1 018.9	806.5	667.0	541.1	398.9	273.8

将表 4 中的数据代入式(29),可以得到增益分别为 0.143 MJ/kg,0.124 MJ/kg,0.105 MJ/kg,也随发电功率降低呈减小的趋势。另外与 600 MW 机组相比,1 000 MW 机组由于汽轮机运行参数提高,其各级抽汽温度、压力参数相应提高,各工况增益都大于 600 MW 机组对应工况增益。

文献[1]计算得出 600 MW 机组满负荷时增益为 0.11 MJ/kg。文献[12]在上海外高桥三厂 1 000 MW 机组上通过实验得到,1 000 MW 负荷时增益为 0.130 MJ/kg; 850 MW 负荷时,增益在 0.072 ~ 0.109 MJ/kg之间。文献[13]在 660 MW 超超临界火电机组上通过实验得到凝结水流量变化量与机组负荷变化量成比例变化的结论,并给出数值,在 499.8 MW 负荷时增益为 0.109 MJ/kg,在 597.6 MW 负荷时,增益为 0.116 MJ/kg。其结果都与本文结论相符。

3 蓄能容量分析

凝结水系统的蓄能容量受凝汽器水箱水位和除氧器水箱水位的限制[14]。因为凝汽器水箱容积较大且对水位的要求不严格,所以一般情况下凝结水系统的蓄能量主要受限于除氧器水箱水位[15]。

PS 电厂 600 MW 机组的除氧器水箱型号为 YYX -230,有效容积为 230 m^3,高报警水位 2 470 mm,正常水位 2 300 mm,低报警水位 1 790 mm,长度 32 000 mm,计算约有 58 m^3 的水容积可以利用。为安全起见,工程中投入凝结水系统蓄能补偿,变化量取 ±50%。假设利用此容积的一半,根据表 5 中不同工况下的参数,得出凝结水系统总的蓄能容量。

表 5 600 MW 机组蓄能容量计算结果

Tab. 5 Calculation results of the energy storage capacity of a 600 MW unit

设计参数	100% THA	75% THA	50% THA
Q_{cw}/kg·s^{-1}	2473	1883	1289
Q_{fw}/kg·s^{-1}	6484	4810	3193
$Q_{sw,3}$/kg·s^{-1}	1238	832	482
ρ/kg·m^{-3}	896	907	920
T/s	121	163	243
C/MJ	2 494	2 302	1 914

ZX 电厂 1 000 MW 机组的除氧器水箱型号为 YS -290,有效容积为 295 m^3,高报警水位 1 230 mm,正常水位 1 030 mm,低报警水位 610 mm,长度为 33 615 mm,计算约有 60 m^3 的水容积可以利用。假设利用此容积的一半,根据表 6 中不同工况下的参数,得出凝结水系统总的蓄能容量。

表 6 1 000 MW 机组蓄能容量计算结果

Tab. 6 Calculation results of the energy storage capacity of a 1 000 MW unit

设计参数	100% THA	70% THA	50% THA
Q_{cw}/kg·s^{-1}	3 737	2 610	1 890
Q_{fw}/kg·s^{-1}	9 839	6 602	4 644
$Q_{sw,3}$/kg·s^{-1}	2 041	1 174	727
ρ/kg·m^{-3}	885	900	913
T/s	85	124	175
C/MJ	3 241	2 940	2 453

表中:ρ—除氧器内水的密度,kg/m^3; T—除氧器内可以利用的水容积维持给水泵正常工作的时间,s; C—凝结水系统可释放的总蓄能容量,MJ。

4 结 论

本文对回热加热系统中低压加热器、除氧器和高压加热器质量 - 能量平衡过程进行机理分析,参考等效焓降法分析凝结水系统凝结水流量变化与机组发电功率变化之间的静态对应关系,并结合 600 MW、1 000 MW 典型机组给出计算实例,得到以下结论:

(1) 依据质量 - 能量守恒定律并结合等效焓降法计算出凝结水流量变化与机组功率变化之间的静态对应关系,具有较高准确度;

(2) 同一机组凝结水系统蓄能容量随负荷增加而增加;

(3) 运行参数越高的机组凝结水系统的蓄能容量越大。

参考文献:

[1] 刘鑫屏,田 亮,曾德良,等. 凝结水节流参与机组负荷调节过程建模与分析[J]. 华北电力大学学报: 自然科学版,2009,36(2):80 -84.

LIU Xin-ping，TIAN Liang，ZENG De-liang，et al. Modeling and analysis of the load regulation process of a unit participated by the condensate water throttling [J]. Journal of North China University of Electric Power：Natural Science Edition，2009，36(2)：80－84.

[2] 闫水保，魏新利，马新灵，等. 加热单元凝结水流量平衡方程及其应用 [J]. 中国电机工程学报，2007，27(20)：99－101.
YAN Shui-bao，WEI Xin-li，MA Xin-ling，et al. Condensate water balance equation for heating units and its applications [J]. Proceedings of China Electric Machinery Engineering，2007，27(20)：99－101.

[3] 刘鑫屏，田　亮，王　琪，等. 供热机组发电负荷－机前压力－抽汽压力简化非线性动态模型 [J]. 动力工程学报，2014，34(2)：115－121.
LIU Xin-ping，TIAN Liang，WANG Qi，et al. Simplified nonlinear dynamic model for the power generation load-pressure before a heat supply unit-its extraction pressure [J]. Journal of Power Engineering，2014，34(2)：115－121.

[4] 邓拓宇，田　亮，刘吉臻. 超超临界直流锅炉蓄热能力的定量分析 [J]. 动力工程学报，2012，32(1)：10－14.
DENG Tuo-yu，TIAN Liang，LIU Ji-zhen. Quantitative analysis of the heat storage capacity of an ultra-supercritical once-through boiler [J]. Journal of Power Engineering，2012，32(1)：10－14.

[5] 姚　峻，陈维和. 900 MW 超临界机组一次调频试验研究 [J]. 华东电力，2006，34(8)：84－87.
YAO Jun，CHEN Wei-he. Experimental study of the primary frequency regulation of a 900 MW supercritical unit [J]. East China Electric Power，2006，34(8)：84－87.

[6] 钱　能，金生祥，王　琪，等. 凝结水节流控制与经济效益分析 [J]. 中国电力，2014，47(3)：69－73.
QIAN Neng，JIN Sheng-xiang，WANG Qi，et al. Condensate water throttling control and its economic benefit analysis [J]. China Electric Power，2014，47(3)：69－73.

[7] 林万超. 火电厂热力系统节能理论 [M]. 西安：西安交通大学出版社，1994：6－21.
LIN Wan-chao. Energy saving theory for thermal systems in thermal power plants [M]. Xi'an：Xi'an Jiaotong University Press，1994：6－21.

[8] 郭民臣，魏　楠，刘文毅. 汽耗变换系数及抽汽等效焓降与主循环的汽耗率 [J]. 中国电机工程学报，2002，22(2)：93－98.
GUO Min-chen，WEI Nan，LIU Wen-yi. Steam rate conversion coefficient，equivalent enthalpy drop of steam extractied and the steam rate of the main cycle [J]. Proceedings of China Electric Machinery Engineering，2002，22(2)：93－98.

[9] 王松岭，张学镭，陈海平，等. 抽汽压损对机组热经济性影响的通用计算模型 [J]. 动力工程，2006，26(6)：888－893.
WANG Song-ling，ZHANG Xue-lei，CHEN Hai-ping，et al. A general-purpose model for calculating the influence of the pressure loss of steam extracted on the thermal cost-effectiveness of a unit [J]. Journal of Power Engineering，2006，26(6)：888－893.

[10] 郭民臣，魏　楠. 电厂热力系统矩阵热平衡方程式及其应用 [J]. 动力工程，2002，22(2)：1733－1738.
GUO Min-chen，WEI Nan. Matrix thermal balance equation formula for thermal systems in power plants and its applications [J]. Journal of Power Engineering，2002，22(2)：1733－1738.

[11] 王承亮. 1 000 MW 机组凝结水系统优化改造研究 [J]. 中国电力，2013，46(12)：48－51.
WANG Cheng-liang. Study of the optimization and modification of the condensate water syutem in a 1 000 MW unit [J]. China Electric Power，2013，46(12)：48－51.

[12] 姚　峻，祝建飞，金　峰. 1 000 MW 机组节能型协调控制系统的设计与应用 [J]. 中国电力，2010，43(6)：79－84.
YAO Jun，ZHU Jian-fei，JIN Feng. Design and application of the energy-saving type coordination control system in a 1 000 MW unit [J]. China Electric Power，2010，43(6)：79－84.

[13] 张　宝，童小忠，吴文健，等. 一种热力发电机组凝结水节流调频负荷特性评估方法：中国，201210039965.2 [P]. 2014－12－10.
ZHANG Bao，TONG Xiao-zhong，WU Wen-jian，et al. A method for evaluating the condensate water throttling and frequency modulation load characteristics of a thermal power generation unit [P]. China：201210039965.2，2014－12－10.

[14] 张　宝，樊印龙，吴文健，等. 凝结水泵变速运行参数的定量计算 [J]. 动力工程学报，2010，30(9)：684－688.
ZHANG Bao，FAN Yin-long，WU Wen-jian，et al. Quantitative calculation of the variable speed operation parameters of a condensate water pump [J]. Journal of Power Engineering，2010，30(9)：684－688.

[15] 程伟良，夏国栋，周　茵，等. 凝结水泵的最佳调节方案分析 [J]. 动力工程，2004，24(5)：739－742.
CHENG Wei-liang，XIA Guo-dong，ZHOU Yin，et al. Analysis of a scheme for optimally controlling a condensate water pump [J]. Power Engineering，2004，24(5)：739－742.

（刘　瑶　编辑）

XU Wen-feng, FU Wen-guang (College of Marine Engineering, Dalian Maritime University, Dalian, China, Post Code: 116026) //Journal of Engineering for Thermal Energy & Power. -2016, 31(7). -47 ~ 54

The stator blades in the last stage of a highly-loaded fan are characterized by their specific features such as a high load, a complicated flow and serious flow separation. To study their aerodynamic performance, flow guiding blades were additionally installed before the stator cascade to simulate the parameters of the gas flow at the outlet of rotor blades in a multi-stage fan. Through rotating the guide blades to change the gas flow angle at their inlet, the aerodynamic characteristics of the stator blades at various gas flow angles at the inlet and under different Mach numbers at the inlet were analyzed. It has been found that the guide blades such designed can provide the parameters of the coming flow close to the conditions at the outlet of the rotor blades in the stage, thus capable of performing an experimental study of the stator blades. These stator blades can form a diffusion cascade with a large turning angle and with an increase of the Mach number, the total pressure recovery coefficient will decrease. With an increase of the turning angle, the flow on the pressure side of the stator blades will obviously improve and the separation area will diminish. The suction surface of the stator blades has a relatively large area being subject to flow separation and an increase of the turning angle of the cascade has no big influence on the flow separation area. **Key words:** fan, stator blade, sector-shaped cascade, experiment

燃气轮机发电模块转速控制策略半物理仿真研究 = Semi-physic Simulation Study of the Rotating Speed Control of the Power Generation Module in a Gas Turbine 附,汉 WANG Guan-lin (China Petroleum Western Pipeline Co., Urumchi, China, Post Code: 830011) //Journal of Engineering for Thermal Energy & Power. -2016,31(7). -55 ~ 61

With the power generation module in a three-shaft gas turbine serving as the object of study and the three-shaft gas turbine as the primer mover, a twelve-phase synchronous power generator serves as the energy conversion device to give a power output to the outside world. Through a Matlab\Simulink simulation platform, a model for simulating power generation modules was established and on the basis of a Rockwell PLC control system and a ADI simulation system, a semi-physic simulation platform was also set up as necessary to simulate and study the dynamic characteristics of power generation modules and formulate the rotating speed control strategies for the power generation modules in various operation states. Furthermore, a simulation and study were made of various conditions of the power generation module in the gas turbine when the load underwent an abrupt change under various operating conditions and the control quality of several rotating speed control versions were analyzed and compared when the power generation module was in various operating states and in combination with the merits of the control versions above-mentioned, optimum rotating speed control strategies were worked out. **Key words:** three-shaft gas turbine, power generation module, load variation, rotating speed control, semi-physic simulation

利用抽汽蓄能提高机组调频能力的定量分析 = Quantitative Analysis of the Enhancement in the Frequency

Modulation Ability of a Unit by Utilizing the Steam Extraction and Energy Storage 刊,汉 ZHANG Rui-feng (Guizhou Electric Power Experiment Research Institute, Guiyang, China, Post Code: 550002), LIAN Hai-qing, TIAN Liang (College of Control and Computer Engineering, North China University of Electric Power, Baoding, China, Post Code: 071003) //Journal of Engineering for Thermal Energy & Power. -2016, 31(7). -62~67

To rationally utilize the energy storage capacity of a condensate water system is capable of enhancing the response speed of a unit in power generation load and to quantitatively analyze its energy storage capacity is of major importance for optimally designing a control system and ensuring a safe operation of the unit. According to the mass and energy conservation law and in combination with the equivalent enthalpy drop method, the correlation of changes in condensate water flow rate with the steam extraction flow rates to various heaters, specific enthalpy and changes in the power of the steam turbine was calculated. Afterwards, according to the volume of the deaerator, the total amount of energy stored was calculated. The calculation results of a 600 MW and 1000 MW typical unit show that the method in question enjoys a relatively high precision. The energy storage capacity of the condensate water system in a same unit will increase with an increase of the load. The higher the operating parameters of a unit, the larger the energy storage capacity of its condensate water system. **Key words:** thermal power generator unit, condensate water system, energy storage capacity, load regulation, enthalpy drop

富氧燃烧氛围下纯煤掺烧生物质的污染物排放模拟研究 = Simulation Study of the Pollutant Emissions During the Combustion of Pure Coal Diluted and Mixed with Biomass in the Oxygen-enriched Combustion Atmosphere 刊,汉 DONG Jing-lan (Education Ministry Key Laboratory on Power Plant Equipment Monitoring and Control, College of Power and Mechanical Engineering, North China University of Electric Power, Baoding, China, Post Code: 071003) //Journal of Engineering for Thermal Energy & Power. -2016, 31(7). -68~73

By making use of the flow path simulation software Asepn Plus, simulated and analyzed were the emission characteristics of pollutants during the combustion of pure coal diluted and mixed with biomass in the oxygen-enriched combustion atmosphere. It has been found that when the dilution and mixing combustion proportion is constant, the NO_x and SO_x emissions concentrations in the flue gases in the oxygen-enriched combustion atmosphere will be far lower than the value in the conventional air combustion atmosphere and the CO emissions concentration, however, will be notably higher than that in the conventional air combustion atmosphere. In addition, with an increase of the O_2 concentration, the NO_x and SO_x emissions concentrations will gradually increase and the CO emissions concentration will decrease step by step. When the O_2 concentration is constant, the combustion temperature has a very big influence on the CO emissions concentration. When the combustion temperature exceeds 1 200 ℃, the CO emissions concentration will increase drastically and the NO_x emissions concentration will increase with an increase of the combustion temperature. The combustion temperature will have no big influence on the SO_x emissions concentration and the latter will somewhat increase with an increase of the combustion temperature. **Key words:** Asepn Plus, oxygen-enriched combustion, diluted and mixed combustion, pollutant